Osteoprotegerin: a double-edged sword in osteoarthritis development

Rodriguez Ruiz, A.

CHAPTER 3

Cartilage from human induced pluripotent stem cells: comparison with neo-cartilage from chondrocytes and bone marrow mesenchymal stromal cells

Alejandro Rodríguez Ruiz[1], Amanda Dicks[2], Margo Tuerlings[1], Koen Schepers[3], Melissa van Pel[3,4], Rob GHH Nelissen[5], Christian Freund[6,7], Christine Mummery[6,7], Valeria Orlova[6], Farshid Guilak[2], Ingrid Meulenbelt[1], and Yolande FM Ramos[1]

[1]Dept. of Biomedical Data Sciences, Section Molecular Epidemiology, Leiden University Medical Center, LUMC, Leiden, The Netherlands; [2]Dept. Orthopedic Surgery, Washington University and Shriners Hospitals for Children, St. Louis, USA; [3]Dept. Immunohematology and Blood transfusion, LUMC; [4]NECSTGEN, Leiden, The Netherlands; [5]Dept. Orthopaedics, LUMC; [6]Dept. Anatomy, LUMC; [7]LUMC hiPSC Hotel.

Cell and Tissue Research. 2021 Nov;386(2):309-320.

ABSTRACT:

Objectives: Cartilage has little intrinsic capacity for repair, so transplantation of exogenous cartilage cells is considered a realistic option for cartilage regeneration. We explored whether human-induced pluripotent stem cells (hiPSCs) could represent such unlimited cell sources for neo-cartilage comparable to human primary articular chondrocytes (hPACs) or human bone marrow derived mesenchymal stromal cells (hBMSCs).

Methods: Chondroprogenitor cells (hiCPCs) and hiPSC-derived mesenchymal stromal cells (hiMSCs) were generated from two independent hiPSC lines and characterized by morphology, fow cytometry, and differentiation potential. Chondrogenesis was compared to hBMSCs and hPACs by histology, immunohistochemistry, and RT-qPCR, while similarities were estimated based on Pearson correlations using a panel of 20 relevant genes.

Results: Our data show successful differentiations of hiPSC into hiMSCs and hiCPCs. Characteristic hBMSC markers were shared between hBMSCs and hiMSCs, with the exception of CD146 and CD45. However, neo-cartilage generated from hiMSCs showed low resemblances when compared to hBMSCs (53%) and hPACs (39%) characterized by lower collagen type 2 and higher collagen type 1 expression. Contrarily, hiCPC neo-cartilage generated neo-cartilage more similar to hPACs (65%), with stronger expression of matrix deposition markers.

Conclusion: Our study shows that taking a stepwise approach to generate neo-cartilage from hiPSCs via chondroprogenitor cells results in strong similarities to neo-cartilage of hPACs within 3 weeks following chondrogenesis, making them a potential candidate for regenerative therapies. Contrarily, neo-cartilage deposited by hiMSCs seems more prone to hypertrophic characteristics compared to hPACs. We therefore compared chondrocytes derived from hiMSCs and hiCPCs with hPACs and hBMSCs to outline similarities and differences between their neo-cartilage and establish their potential suitability for regenerative medicine and disease modelling.

Key messages:

- Neo-cartilage deposited from hiCPCs is 65% similar to hPAC neo-cartilage with stronger expression of matrix deposition markers.
- Neo-cartilage deposited from hiMSCs shows a 53% similarity to hBMSCs with higher expression of hypertrophic markers.

INTRODUCTION

Articular cartilage, the smooth and lubricated tissue lining the end of long bones, plays an important role in mobility by ensuring frictionless articulation while withstanding compressive forces during joint loading. It is composed entirely of chondrocytes, responsible for maintaining tissue homeostasis upon stress, by synthesizing a dense cartilage extracellular matrix (ECM), rich in collagens, proteoglycans, and sulphated glycosaminoglycans (s-GAGs) (1, 2). However, due to a lack of blood supply or lymphatic vessels, cartilage is essentially unable to regenerate, contributing to development of diseases such as osteoarthritis (OA) (3, 4) and making cartilage regeneration therapies essential to fighting this debilitating condition. Some therapies, based on administering human primary articular chondrocytes (hPACs) and/or mesenchymal stromal cells (MSCs), have been shown to produce stable and healthy neo-cartilage that can be used in implants and for *in vitro* disease models (5-7).

Previously, we showed the potential of hPAC-derived neo-cartilage for cartilage regeneration based on their 99% similarity of genome-wide methylation to autologous cartilage (8). While autologous neo-cartilage would avoid the immunogenic response that allogenic cells may cause, this technique is relatively invasive for patients since, prior to implantation, a biopsy of the articular cartilage is needed. Alternatively, MSCs can be obtained from several tissues and have the potential to differentiate into relevant cells. Nonetheless, the procedure to obtain them is still invasive, and has a large variability in differentiation efficiency and early senescence in *in vitro* cultures (7, 9, 10).

Human induced pluripotent stem cells (hiPSCs) have been proposed to provide an excellent alternative for both cartilage regeneration and disease modeling applications (11). Firstly, their production can be scaled, circumventing restrictions in defect size for treatments in the clinic and during disease modeling. Secondly, the use of a cell line circumvents the need for biopsies and thus repeated surgeries on patients. Finally, hiPSCs can be genetically modified to increase chondrogenic potential, introduce patient specific mutations for research purposes, and/or reduce their immunogenicity. Nonetheless, obtaining good quality neo-cartilage from hiPSCs has so far proven challenging.

Issues arise due to the strong variation in differentiation efficiencies between hiPSC lines and clones and a tendency to generate hypertrophic and fibrous matrix (7, 12). Hence, even though several protocols are available, the optimal method for the generation of chondrocytes from hiPSCs remains to be established. Some studies comparing human bone marrow-derived mesenchymal stromal cells (hBMSCs) and hiPSC-derived mesenchymal stromal cells (hiMSCs) suggest major functional and genetic differences, not only between cells but also between neo-

cartilage from both cell types (13, 14). However, in these studies, hiMSCs were generated via the formation of cell aggregates called embryoid bodies (EBs), often variable and with low efficiency (13, 14) while direct monolayer generation was shown to be more robust (15).

Alternatively, a stepwise approach could be taken to generate neo-cartilage from hiPSCs via human chondroprogenitor cells (hiCPCs) (16-18). Notably, differentiation of hiPSCs with this protocol optimizes each developmental step through anterior primitive streak formation and successive emergence of hiCPCs, diminishing variability between independent differentiations. Unfortunately, a major disadvantage of this method is the inefficiency to expand hiCPCs, mainly due to the rapid loss of their chondrogenic potential within a few passages (17).

Here, we aimed to assess upon both approaches towards consistent generation of neo-cartilage from hiPSC with characteristics similar to chondrocytes from hPACS and hBMSCs (the 'gold standard'). We therefore compared chondrocytes derived from hiMSCs and hiCPCs with hPACs and hBMSCs to outline similarities and differences between their neo-cartilage and establish their potential suitability for regenerative medicine and disease modelling.

MATERIALS AND METHODS

Tissue culture and chondrogenesis

Cell culture of hiPSCs and primary cells

Two independent control hiPSC lines were used in the current study. Approval for the generation of hiPSCs from skin fibroblasts of healthy donors is available under number P13.080. Cells were generated from skin fibroblasts of a female: LUMC0030iCTRL12 (030) and a male: LUMC0004iCTRL10 (004) by the LUMC hiPSC core facility and registered at the Human pluripotent stem cell registry. Cells were characterized according to pluripotent potential and spontaneous differentiation capacity by the hiPSC core facility (20) and were karyotyped after 15 passages in culture.

hiPSCs were maintained under standard conditions (37°C, 5% CO_2) in TeSR-E8 medium (STEMCELL Technologies) on VitronectinXF-coated plates (STEMCELL Technologies). The medium was refreshed daily and cells were passaged in aggregates using Gentle Cell Dissociation Reagent (STEMCELL Technologies) upon reaching approximately 80% confluency. Human BMSCs and hPACs were collected from OA patients undergoing joint replacement surgery as part of the RAAK study. Collection and expansion of the primary cells has been previously described (8). Cells were counted with the Nucleocounter NC-200 (Chemometec).

Differentiation of hiPSC towards hiMSCs and hiCPCs

Human iMSCs were generated using the Stemcell Technologies Mesenchymal Progenitor Kit following the manufacturers' instructions with small modifications. Following three passages using the recommended Mesencult ACF plus medium, cells were grown in DMEM high glucose (Gibco) supplemented with 10% fetal calf serum (FCS; Biowest), basic FGF (bFGF; 5ng/ml; Life Technologies), and antibiotics (100U/ml penicillin, 100µg/ml streptomycin; Gibco) until elongated and with fibroblast-like morphology. At passage 5, MSC surface markers were analyzed by flow cytometry, and the trilineage potential of the hiMSCs was determined. Generation of hiCPCs was performed as described previously (17). At day 14, analysis for cell surface markers was performed, and hiCPC aggregates were collected for chondrogenesis (**Supplementary Figure 1**).

Multilineage Differentiations

For adipogenesis, $1.5x10^4$ cells/cm^2 were seeded on tissue culture-treated 6-well plates (Cellstar), and differentiation was induced in α-MEM (Gibco) supplemented with 10% FCS, antibiotics, dexamethasone (0.25µM; Sigma-Aldrich), L-ascorbate-2-phosphate (50µg/ml; Sigma-Aldrich), insulin (100µg/ml; Sigma-Aldrich), indomethacin (50µM; Sigma-Aldrich), and 1-methyl-3-isobutylxantine (0.5mM; Sigma-Aldrich). Medium was refreshed twice a week for 21 days.

Chondrogenesis was performed in 3D cell pellets following our established protocol (21). In short, cell pellets (hBMSCs, hiMSCs, hPACs) were maintained in DMEM high glucose (Gibco) supplemented with 1% ITS-plus (Corning), dexamethasone (100nM), L-ascorbate-2-phosphate (50µg/ml), L-proline (40µg/ml; Sigma-Aldrich), sodium pyruvate (100µg/ml; Sigma-Aldrich), TGF-β1 (10ng/ml; PeproTech), and antibiotics. The medium was refreshed every 3–4 days. Chondrogenesis for hiCPCs was performed basically as described by Dicks *et al. [17]:* cell aggregates were maintained in DMEM/F-12 (Gibco) supplemented with 1% ITS-plus, 2-Mercaptoethanol (55µM; Gibco), dexamethasone (100nM), 1% non-essential amino acids (NEAA; Gibco), L-ascorbate-2-phosphate (50µg/ml), L-proline (40µg/ml), TGF-β1 (10ng/ml), and antibiotics, for 21 days while refreshing medium every 3-4 days. Note that due to their initial stem cell state, hBMSCs and hiMSCs require an extended period for chondrogenesis and deposition of mature cartilage ECM (35 days) as compared to hPACs and hiCPCs (21 days).

Osteogenesis was induced by maintaining day-21 chondrogenic pellets for an additional 14 days with α-MEM supplemented with 10% heat-inactivated FCS, dexamethasone (0.1µM), L-ascorbate-2-phosphate (50µg/ml), b-Glycerophosphate (5mM; Sigma-Aldrich), and antibiotics.

Flow cytometric analyses

Human BMSCs and hiMSCs were analyzed for the following panel of surface markers: CD31, CD45, CD73, CD90, CD105, CD146, and CD166 (BD Biosciences). Human iCPCs were analyzed for CD45, CD90, CD146, and CD166. LIVE/DEAD fixable Aqua Dead Cell stain kit (Thermofisher) was used to define dead cells, and OneComp ebeads (Thermofisher) were used to compensate for the fluorochromes. Data were obtained using the BD LSR-II Flow Cytometer and analyzed with FlowJo 6.0 software.

RNA isolation and RT-qPCR

Differentiations with hiPSC lines were performed in triplicate. For RNA isolations, two pellets were pooled, and isolation was performed as described previously (21). Total mRNA (150 ng) was processed with a first strand cDNA kit according to the manufacturer's protocol (Roche Applied Science). cDNA was further diluted five times, and preamplification with TaqMan preamp master mix (Thermo Fisher Scientific Inc.) was performed for a panel of 20 designated genes related to chondrogenesis, hypertrophy, deposition and degradation of cartilage ECM, and neo-cartilage quality (primer sequences in **Supplementary Table S1**). Gene expression was measured with a Fluidigm Biomark HD machine using a 96.96 IFC chip. Quality control of the data was performed, and non-detected values were imputed according to the minimum detected value. Unsuccessful differentiations, defined by the minimum detected expression of *COL2A1* for hPACs and hBMSCs neo-cartilage, were disregarded.

Histology and immunohistochemistry

Tissues (neo-cartilage and neo-bone) were fixed in 4% formaldehyde and embedded in paraffin. After sectioning, slides were deparaffinized and rehydrated prior to histology or immunohistochemistry.

Overall cellular and tissue structure was visualized with hematoxylin-eosin (HE) staining. Glycosaminoglycans were visualized by staining with 1% Alcian Blue 8-GX (Sigma-Aldrich) and Nuclear Fast red staining (Sigma-Aldrich). Calcium deposits were stained with 2% Alizarin Red S (Sigma-Aldrich).

To detect COL2 (MAB1330; Millipore; 1:100 in TBST/10% normal goat serum, overnight at 4°C), COL1 (ab34710; Abcam; 1:1000 in TBST/10% normal goat serum, overnight at 4°C), and COL10 (x53/2031501005; Quartett; 1:100 in TBST/10% normal goat serum, overnight at 4°C), immunohistochemistry was performed with 3-diaminobenzidine (DAB) solution (Sigma-Aldrich) and hematoxylin (Klinipath) as described before (21).

Lipid droplets were stained for 10 minutes with Oil-Red-O solution (Sigma-Aldrich) after fixation of the cells in 4% formaldehyde. To reduce the background, the following staining cells were gently washed with 60% isopropanol and distilled water.

Statistics and similarities

Relative gene expression (−ΔCt values) were calculated using levels of glyceraldehyde 3-phosphate dehydrogenase (*GAPDH*) and acidic ribosomal phosphoprotein P0 (*ARP*) as housekeeping genes. Betas, standard errors (SE), and P-values for gene expression differences across cell types were determined by applying generalized estimation equations (GEE; IBM SPSS software). P-values <0.05 were considered statistically significant.

Similarities between the different cell types and differentiations were calculated based on Pearson correlations using a panel of 20 relevant genes.

RESULTS

Generation and characterization of hiMSCs

Two independent control hiPSC lines, well-characterized by morphology, pluripotent status, spontaneous differentiation capacity, and by karyotyping, were used for this study (**Supplementary Figure S2** and Ref. (20)). Cells were differentiated towards hiMSCs and compared to hBMSCs after five passages. Expression of typical MSC surface markers as defined by the International Society of Cellular Therapy (ISCT: presence of CD73, CD90, CD105; absence of CD31, CD45 (22)) and expression of CD146 and CD166 (expressed in chondroprogenitor cells (18)) were assessed by flow cytometry (**Figure 1a-b**). Highly comparable expression was observed for CD73, CD90, CD105, and CD166 between hiMSCs and hBMSCs, while cells were negative for CD31. Significant differences, however, were found for CD146 and CD45. Both markers were expressed in a larger percentage of the hiMSC population compared to 44% and 9% in hBMSCs, respectively (CD146: for hiMSC-030 and hiMSC-004 resp. 98% and 96%, P-value=$3.06\text{x}10^{-7}$ and $1.39\text{x}10^{-6}$; CD45: for hiMSC-030 and hiMSC-004 resp. 29% and 28% with P-value=$1.38\text{x}10^{-9}$ and $0\text{x}10^{-0}$). **Figure 1c-1d** shows morphology of hiMSCs, with majority of the cells being spindle-shaped, elongated, and fibroblast-like. Importantly, hiMSCs showed tri-lineage differentiation into fat (Oil red, **Fig c'-d'**), bone (Alizarin red, **Fig c''-d''**), and cartilage (Alcian blue, **Fig c'''-d'''**), as confirmed by histology. Altogether, our analyses confirmed successful differentiation of hiPSCs into a mesenchymal stromal cell type.

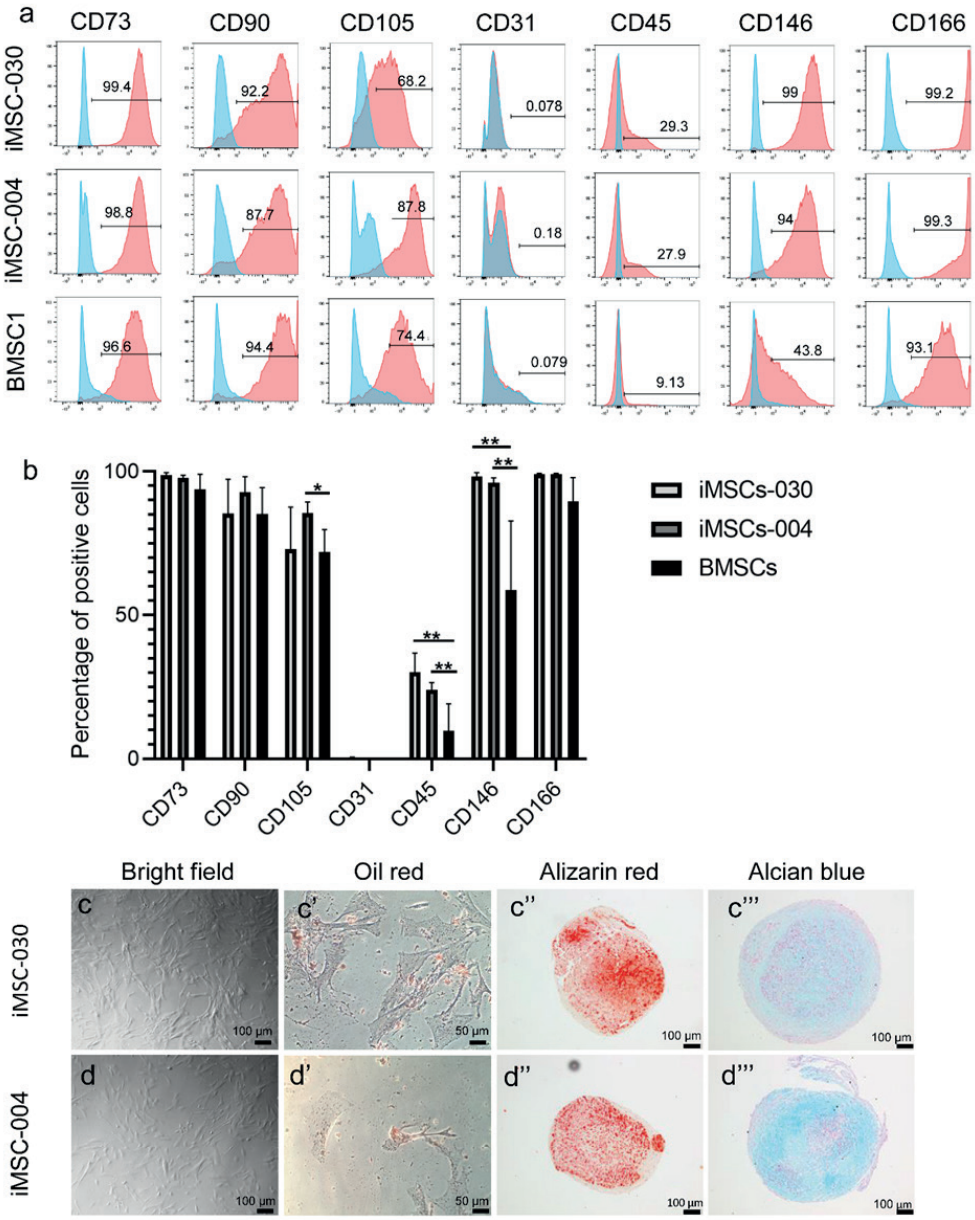

Figure 1. Characterization of hiMSCs. a-b) Flow cytometry analysis of MSC characteristic markers. The blue histogram shows unstained cells, while the red histogram shows specific marker cell staining. Results shown are the average of three independent differentiations with their standard deviation for each hiPSC line and for three hBMSC lines (hiMSC-030: CD146: **P-value= $3.06x10^{-7}$ and CD45, **P-value=$5.93x10^{-10}$; hiMSC-004: CD146, **P-value=$1.39x10^{-6}$; CD45, **P-value=$0x10^{-0}$ and CD105, *P-value=$4.18x10^{-4}$). **c-d**) Bright field microscopy image of hiMSCs and representative images for trilineage differentiation. Human iMSCs show a fibroblastic and spindle-shaped morphology (**c-**

d); adipocytes were stained by Oil red (**c'-d'**), osteocytes by Alizarin red (**c''-d''**), and chondrocytes by Alcian blue (**c'''-d'''**).

Generation and characterization of hiCPCs

Control hiPSCs were differentiated towards hiCPCs. After 14 days, analysis of cell surface markers showed similar expression of CD45, CD90, and CD166 across both hiPSC lines (**Figure 2a-b-c**). However, CD146 was expressed within a lower percentage of hiCPC-030 as compared to hiCPC-004 (10% versus 20%, P-value=$5.1x10^{-3}$). Notably, overall percentages of CD90, CD146, and CD166 positive cells appeared smaller than compared to the hiMSCs, while the percentage of CD45-positive hiCPCs was relatively large (38% and 25% among hiCPCs-004 and hiCPCs-030, respectively). **Figure 2d** shows cell morphology, indicating population heterogeneity and spontaneous cell aggregation as arises during the hiCPC-generating process.

Histochemistry analysis of neo-cartilage

Prior to quantitative gene expression analyses, general neo-cartilage pellet formation and cellular structures of hiMSCs and hiCPCs was compared to that of hBMSCs and hPACs by HE and Alcian Blue staining. Following 35 days of chondrogenesis, HE staining of hiMSC neo-cartilage showed the presence of a core with higher number of cells, concurrent with less matrix as compared to hBMSC-derived neo-cartilage (**Figure 3a-f**). Yet, the presence of lacunae can be observed in the hiMSC neo-cartilage, indicating successful generation of cartilage ECM as also confirmed by the Alcian Blue staining (**Figure 3b-g**). To reduce heterogeneity of hiCPC population, 3D pellets were generated starting from cell aggregates (such as indicated in **Figure 2d-d'**). HE staining showed relatively homogeneous ECM deposition, lacunae formation, but also off-target cells on the outer surface of some hiCPC pellets (**Figure 3f'**, hiCPC-004). When comparing hiCPC- and hPAC-derived neo-cartilage, Alcian Blue staining seemed more intense and homogenous as compared to that of hiMSCs and hBMSCs (compare **Figure 3b-b''** and **3g-g''**).

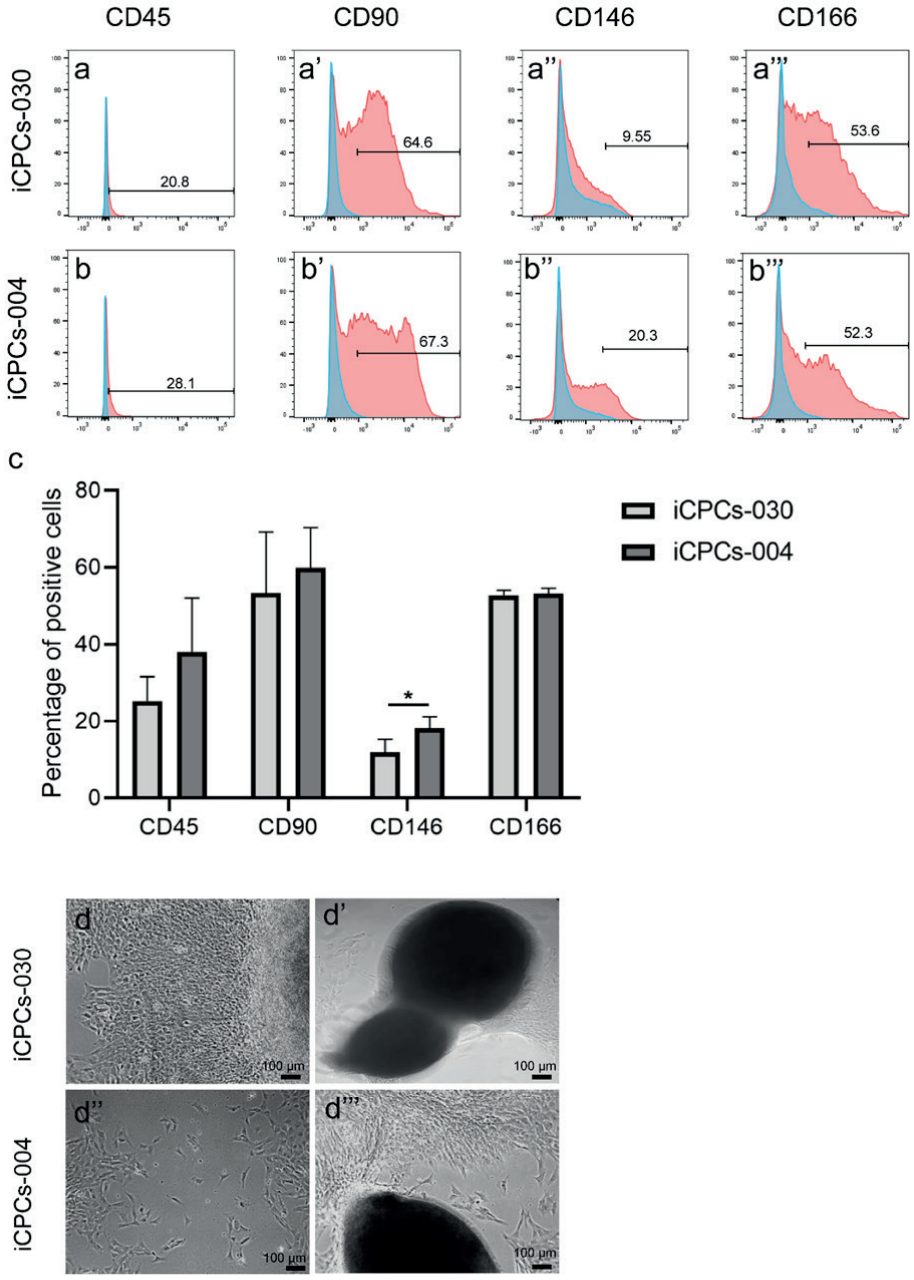

Figure 2. Characterization of hiCPCs. a, b, c) Flow cytometry analysis of CD45, CD90, CD146, and CD166 for hiCPCs. Results shown are the average of independent differentiations for each hiPSC line (n=2, *P-value=5.1x10^{-3}). **d**) Bright field microscopy image of hiCPCs showing cells growing in monolayer and cell aggregates following 14 days in differentiation.

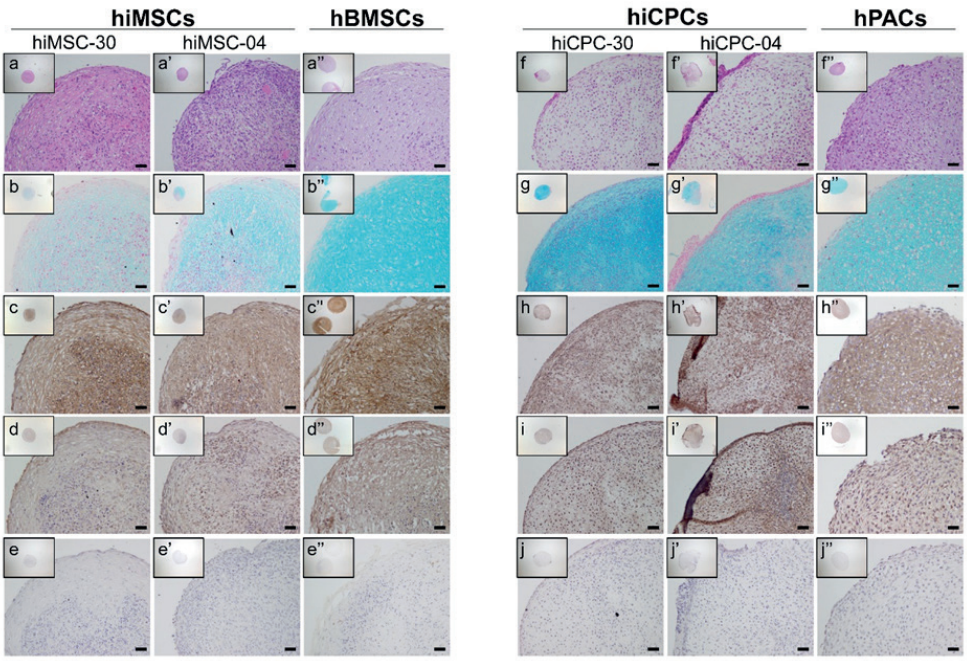

Figure 3. Histology and immunohistochemistry of neo-cartilage. Representative images of neo-cartilage generated by hiMSCs and hBMSCs after 35 days of chondrogenesis (**a-e**), or by hiCPCs and hPACs following 21 days of chondrogenesis (**f-j**), stained with H&E (**a** and **f**), Alcian Blue (**b** and **g**), COL1 (**c** and **h**), COL2 (**d** and **i**), and COL10 (**e** and **j**). Scale bars: 50 µm.

Gene expression profiles and immunohistochemistry of hiMSC-, hBMSC-, and hPAC-derived neo-cartilage

To characterize chondrogenesis efficiency, RT-qPCR was performed of hiMSC- and hBMSC-derived neo-cartilage (day 35) and hPAC-derived neo-cartilage (day 21). Fold differences were calculated for chondrocyte-specific genes relative to hBMSCs-derived neo-cartilage (**Table 1** and **Figure 4**). While the expression of *COL2A1* only showed a trend towards lower expression (FD=-17.2, P-value=9.0x10^{-2}), significantly lower levels of matrix gene *ACAN* (FD=-21.8, P-value=1.1x10^{-2}) and chondrogenic transcription factor *SOX9* (FD=-3.9, P-value=2.6x10^{-2}) were expressed in hiMSC-derived neo-cartilage compared to that from hBMSCs. Additionally, in hiMSCs-derived neo-cartilage, *EPAS1* was significantly lower (FD=-5.7, P-value=9.8x10^{-3}), and hypertrophic cartilage marker *COL10A1* was very lowly expressed (FD=-4092.3, P-value=0.0x10^{-0}).

Based on the gene expression profiles, we determined that following 35 days of chondrogenesis, neo-cartilage pellets derived from hiMSCs and hBMSCs were 53% similar (SD=16; see **Supplementary Table S2a** for complete overview

of hiMSC-hBMSC similarities). Since the similarity was not very strong, we questioned whether differentiated hiMSCs were more comparable to hPACs. However, based on the expression profile of our gene panel, we found only 39% similarity (SD=20; see **Supplementary Table S2c** for a complete overview of hiMSC-hPAC similarities). In fact, the majority of the genes here assessed (14 out of 20; **Table 2**) were significantly different expressed between hiMSC- and hPAC-derived neo-cartilage. Specifically, expression of matrix genes such as *COL2A1* (FD=-10.5, P-value=$4.2x10^{-2}$) and *ACAN* (FD=-29.5, P-value=$7.6x10^{-3}$) were lower, while catabolic and mineralization genes such as *MMP13* (FD=123.2, P-value=$1.4x10^{-3}$), *COL1A1* (FD=5.5, P-value=$1.7x10^{-3}$), and *ALPL* (FD=51.7, P-value=$1.4x10^{-3}$) were higher expressed. Altogether, this suggests that during chondrogenesis, hiMSCs deposit neo-cartilage of inferior quality as compared to that of hPACs.

Although inherently less sensitive to gene expression levels, hence less suitable for quantitative analyses, immunohistochemistry of COL1, COL2 and COL10 was performed to allow visualization of protein localization for hBMSC- and hiMSC-derived neo-cartilage. As it can be seen in **Figure 3c-c"**, COL1 in hiMSC-derived neo-cartilage seemed to be particularly localized in the surrounding of cells and at the core of the neo-cartilage pellet, while BMSC-derived neo-cartilage showed a homogeneous staining across the matrix. COL2 staining of hiMSC-derived neo-cartilage as compared to BMSC-derived neo-cartilage showed more variability, while being particularly localized, across all the different cell lines, in the cytoplasm and not in the ECM (**Figure 3d-d"**). With respect to COL10A1 protein expression, staining intensity was generally low similar to the *COL10A1* gene expression (**Figure 3e-e"**).

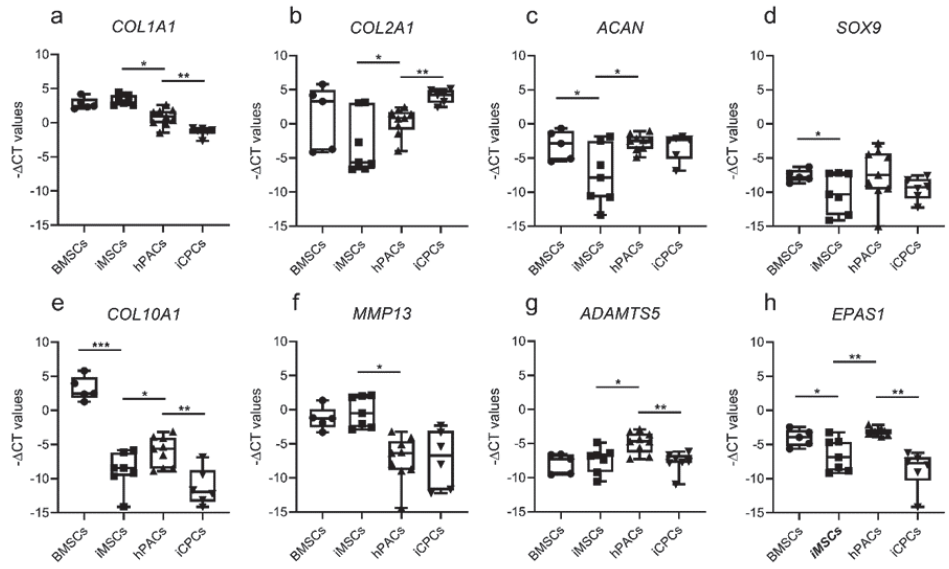

Figure 4. Boxplots for -ΔCt values of matrix, hypertrophy and chondrogenic genes (a-h) as indicated between hiMSCs and hBMSCs, hiMSCs and hiCPCs, and hiCPCs and hPACs, following 35 days (hBMSCs, hiMSCs) and 21 days (hPACs, hiCPCs) of chondrogenesis (n=5-7; * P-value< 0.05; ** P-value< 10^{-4}; *** P-value< 10^{-6}.).

Table 1. Differences in gene expression between hiMSC-and hBMSC-derived neo-cartilage at week 5. Significant data are highlighted in bold.

hiMSCs versus hBMSCs neo-cartilage				
Matrix genes	**FD**	**Beta**	**SE**	**P value**
ACAN	**-21.8**	**-4.4**	**1.7**	**$1.1x10^{-2}$**
COL2A1	-17.2	-4.1	2.4	$9.0x10^{-2}$
COL1A1	1.4	0.5	0.4	$2.7x10^{-1}$
COL10A1	**-4092.3**	**-12.0**	**1.2**	**$0.0x10^{+0}$**
Hypertrophy genes	**FD**	**Beta**	**SE**	**P value**
ADAMTS5	1.4	0.5	0.9	$5.9x10^{-1}$
MMP13	2.0	1.0	1.0	$3.5x10^{-1}$
EPAS1	**-5.7**	**-2.5**	**1.0**	**$9.8x10^{-3}$**
WWP2	-1.2	-0.3	0.3	$2.8x10^{-1}$
ALPL	-3.1	-1.6	1.3	$2.1x10^{-1}$
Chondrogenesis genes	**FD**	**Beta**	**SE**	**P value**
SOX5	-3.9	-2.0	1.3	$1.3x10^{-1}$
SOX6	-2.2	-1.1	0.9	$2.2x10^{-1}$
SOX9	**-3.9**	**-2.4**	**1.1**	**$2.6x10^{-2}$**

	hiMSCs versus hBMSCs neo-cartilage			
FGFR2	**-22.0**	**-4.5**	**1.6**	**$5.9x10^{-3}$**
NOTCH1	1.5	0.6	0.8	$5.0x10^{-1}$
NOTCH3	-2.9	-1.5	0.9	$6.9x10^{-2}$
SMAD3	1.4	0.5	0.5	$3.3x10^{-1}$
SMAD7	1.0	0.0	0.5	$9.7x10^{-1}$
GDF5	1.6	0.2	0.5	$6.4x10^{-1}$
PRG4	-5.0	-0.4	0.7	$6.0x10^{-1}$
NFAT5	**-1.5**	**-0.6**	**0.3**	**$1.9x10^{-2}$**

Characterization of differences between hiCPC- and hPAC-derived neo-cartilage

Subsequently, hiCPC chondrogenesis was characterized. In contrast to hBMSCs, hiCPCs already showed a strong deposition of cartilage ECM at day 21 as determined by Alcian Blue and COL2 staining (**Figure 3g-g"** and **i-i"**). Furthermore, we noticed that, based on expression levels of *COL2A1*, 79% of all hiCPC-derived pellets passed our criterium for deposition of neo-cartilage. Among hiMSC differentiations, however, more variation was observed and fewer pellets (54%) passed the pre-set threshold for expression levels of *COL2A1*.

Gene expression analyses of hiCPC-derived neo-cartilage compared to that of hPACs (**Table 3** and **Figure 4**) demonstrated significantly higher levels of *COL2A1* (FD=13.0, P-value=$5.7x10^{-7}$) and lower expression of genes associated with cartilage hypertrophy, such as *COL10A1* (FD=-35.9, P-value=$5.7x10^{-7}$) and *COL1A1* (FD=-4.3, P-value=$7.7x10^{-6}$). In addition, levels of the catabolic gene *ADAMTS5* were significantly lower (FD=-5.2, P-value=$1.0x10^{-5}$). Together, this indicates enhanced quality of matrix deposited by hiCPCs during chondrogenesis. Comparison of the chondrocyte-specific gene panel showed 65% similarity (SD=12.5) between hiCPC- and hPAC-derived neo-cartilage (see **Supplementary Table S2b** for complete overview of hiCPC-hPAC similarities). Prolonged chondrogenesis of hiCPCs until day 35 did not further improve similarity with hPACs, while expression levels of hypertrophic and mineralization gene *ALPL* significantly increased (FD=4.0, P-value=$1.8x10^{-2}$; **Supplementary Table S3**).

To explore protein localization and matrix structure, COL1, COL2, and COL10 staining was performed for hiCPC- and hPAC-derived neo-cartilage pellets. As can be observed in **Figure 3h"** COL1 staining was consistently expressed throughout the ECM of the hPACs-derived neo-cartilage, while hiCPC-derived pellets (**Figure 3h**) showed a less uniform staining. Expression of COL2 was well-detectable in the hiCPC neo-cartilage throughout the pellets and comparable to

hPAC-derived neo-cartilage (**Figure 3i-i"**). Comparable to hBMSC- and hiMSCs-derived neo-cartilage, only faint COL10 expression in the ECM was observed (**Figure 3j** and **3j"**).

Table 2. Differences in gene expression between hiMSC- and hPAC-derived neo-cartilage at respectively week 5 and 3. Significant data are highlighted in bold.

hiMSCs versus hPACs neo-cartilage				
Matrix genes	**FD**	**Beta**	**SE**	**P value**
ACAN	**-29.5**	**-4.9**	**1.6**	**$7.6x10^{-3}$**
COL2A1	**-10.5**	**-3.4**	**1.7**	**$4.2x10^{-2}$**
COL1A1	**5.5**	**2.5**	**0.5**	**$1.7x10^{-3}$**
COL10A1	**-6.7**	**-2.8**	**1.2**	**$2.0x10^{-2}$**
Hypertrophy genes	**FD**	**Beta**	**SE**	**P value**
ADAMTS5	**-5.9**	**-2.6**	**0.8**	**$1.8x10^{-3}$**
MMP13	**123.2**	**6.9**	**1.3**	**$1.4x10^{-3}$**
EPAS1	**-10.9**	**-3.4**	**0.8**	**$4.8x10^{-5}$**
WWP2	**-2.3**	**-1.2**	**0.4**	**$2.8x10^{-3}$**
ALPL	**51.7**	**5.7**	**1.8**	**$1.4x10^{-3}$**
Chondrogenesis genes	**FD**	**Beta**	**SE**	**P value**
SOX5	**-8.2**	**-3.0**	**1.3**	**$2.3x10^{-2}$**
SOX6	-2.6	-1.4	0.9	$1.5x10^{-1}$
SOX9	-5.4	-2.4	1.7	$1.4x10^{-1}$
FGFR2	**-89.6**	**-6.5**	**1.5**	**$2.1x10^{-5}$**
NOTCH1	-1.1	-0.1	0.7	$8.6x10^{-1}$
NOTCH3	2.0	1.0	0.7	$1.7x10^{-1}$
SMAD3	**-2.4**	**-1.3**	**0.6**	**$2.5x10^{-2}$**
SMAD7	1.6	0.7	0.6	$2.1x10^{-1}$
GDF5	**-22.0**	**-0.7**	**0.2**	**$1.8x10^{-4}$**
PRG4	**-77.7**	**-1.1**	**0.1**	**$3.5x10^{-9}$**
NFAT5	-1.2	-0.2	0.3	$4.3x10^{-1}$

Table 3. Differences in gene expression levels between hiCPC- and hPAC-derived neo-cartilage at week 3 of chondrogenesis. Significant data are highlighted in bold.

hiCPCs versus hPACs neo-cartilage				
Matrix genes	**FD**	**Beta**	**SE**	**P value**
ACAN	-1.6	-0.7	0.8	$4.2x10^{-1}$
COL2A1	**13**	**3.7**	**0.7**	**$5.7x10^{-7}$**
COL1A1	**-4.3**	**-2.1**	**0.5**	**$7.7x10^{-6}$**
COL10A1	**-36**	**-5.2**	**1.2**	**$1.9x10^{-5}$**
Hypertrophy genes	**FD**	**Beta**	**SE**	**P value**
ADAMTS5	**-5.2**	**-2.4**	**0.5**	**$1.0x10^{-5}$**
MMP13	1.0	0.1	1.9	$9.7x10^{-1}$
EPAS1	**-48**	**-5.6**	**1.1**	**$2.1x10^{-7}$**
WWP2	1.0	0.0	0.5	$9.6x10^{-1}$
ALPL	1.8	0.8	1.8	$6.4x10^{-1}$
Chondrogenesis genes	**FD**	**Beta**	**SE**	**P value**
SOX5	1.4	0.5	0.4	$2.4x10^{-1}$
SOX6	-2.3	-1.2	1.4	$3.9x10^{-1}$
SOX9	-3.8	-1.9	1.5	$1.9x10^{-1}$
FGFR2	1.5	0.6	0.5	$2.8x10^{-1}$
NOTCH1	3.1	1.6	0.9	$5.7x10^{-2}$
NOTCH3	1.7	0.8	0.6	$2.1x10^{-1}$
SMAD3	**-8.7**	**-3.1**	**1.0**	**$1.2x10^{-3}$**
SMAD7	-1.9	-0.9	1.4	$5.0x10^{-1}$
GDF5	**-15.7**	**-1.3**	**0.3**	**$5.0x10^{-6}$**
PRG4	**-18.3**	**-0.8**	**0.2**	**$1.0x10^{-6}$**
NFAT5	-1.2	-0.3	0.3	$3.7x10^{-1}$

DISCUSSION

To get more insight into the consistency of frequently used neo-cartilage differentiation protocols for hiPSCs, as well as the resulting neo-cartilage quality, we here compared a stepwise protocol to generate human chondroprogenitor cells (hiCPCs) and hiPSC-derived mesenchymal stromal cells (hiMSCs), then allowed them to undergo chondrogenesis in parallel with human primary chondrocytes (hPACs) and bone marrow mesenchymal stromal cell (hBMSCs) equivalents. The results obtained with our 20-gene chondrocyte-specific gene panel showed almost 70% similarity of hiCPC neo-cartilage when compared with human primary chondrocytes. This stepwise protocol circumvented the need for intermediate cells (hiMSCs), for which we found only 39% similarity to hPACs.

In addition to the relatively high similarity, the advantages of the stepwise approach include the shorter time frame and high efficiency of chondrogenesis. Based on a pre-set threshold for expression levels of *COL2A1,* 79% of the hiCPC pellets deposited good neo-cartilage, while, in line with previous studies (14, 15), chondrogenesis with the hiMSCs was successful in 54% of the pellets. Among others, hiCPC-derived neo-cartilage showed significantly (13-fold) higher expression of *COL2A1* compared to that from hPACs, which was in accordance with the COL2 protein expression as detected with immunohistochemistry. *COL1A1* and *COL10A1* expression were 4.3-fold and 36-fold lower, respectively, than their levels in hPACs. Results of COL1 immunohistochemistry were in line with this, however, for COL10 expression we did not observe pronounced differences across the different cell sources. Furthermore, the expression level of *ADAMTS5* in hiCPC-derived neo-cartilage was found to be 5.2-fold lower than that in hPACs, which may explain the visibly higher Alcian blue intensity, indicative of s-GAG levels in the hiCPC-derived neo-cartilage. Together, our data denote that generation of hiCPC-derived neo-cartilage offers promising prospects for skeletal regenerative therapies with less hypertrophic neo-cartilage; although, further improvement in differentiation efficiency and quality may still be possible and further confirmation of applicability by *in vivo* experiments will be required.

Unfortunately, a major disadvantage of hiCPCs is the reduction of their chondrogenic potential following expansion *in vitro* (17, 18), requiring repeated chondrogenic differentiations to ensure deposition of high quality neo-cartilage. A possible culprit of this, is the generation of a diverse heterogenous hiCPC population, where neurogenic and mesenchymal lineage cells are involved (18, 23). A chondrogenic selection of this population and further optimization of differentiation factors may improve chondrogenic potential and diminish expansion problems while increasing cartilage quality. Such increase in differentiation potential has been demonstrated by Dicks *et al.* when sorting for CD146, CD166, and PDGFRβ surface marker expression or by using a GFP-*COL2A1* reporter hiPSC line. This *COL2A1* marker, however, is known to be expressed in a wide variety of tissues (24). Therefore, another option would be to use a reporter line with an earlier chondrogenic marker, such as *SOX9,* to further enhance the efficiency of the differentiation. This was recently performed for immortalized adipose-derived stem cells with stable *SOX9* overexpression, which showed enhanced chondrogenic potential (25).

Of note was the expression of CD45 in both hiCPC lines, (38% of hiCPC-004 with SD=14 and 25% of the hiCPC-030 with SD=6.3) since CD45 is a transmembrane protein tyrosine phosphatase and a known characteristic of hematopoietic cells (26). It has been found that chondrogenesis in the presence of CD45-positive cells of hematopoietic origin enhanced the expression of chondrogenic genes such as *COL2A1* and *SOX9* (27). Therefore, the CD45-expressing cells within the

mixed population of cells from different lineages that are generated with the stepwise protocol may contribute to enhancing the chondrogenic potential of the cells. This was, however, not observed for the hiMSCs.

Characterization of the hiMSCs showed that the well-known hBMSC surface markers (i.e. CD90, CD105, CD73, CD31, CD166) were similarly expressed across the various differentiations, with exception of CD45 (27% of hiMSCs with SD=6 as compared to 10% of hBMSCs with SD=9) and CD146 (97% of hiMSCs with SD=2 as compared to 59% of hBMSCs with SD=24). CD146 is a transmembrane glycoprotein that belongs to the immunoglobulin superfamily of cell adhesion molecules (CAMs), and is involved in cell adhesion and proliferation (28). Furthermore, it has been described as an excellent multipotency marker for MSCs, as compared to specialized cells (29-31), while showing a direct correlation to chondrogenic potential (32).

Comparison of hiMSC- and BMSC-derived neo-cartilage showed a 53% similarity. Although this is considerable, it should be noted that the hiMSCs from both hiPSC lines and across all differentiations performed do display high levels of heterogeneity, as shown in **Figure 3**. To compensate for this, Diederichs *et al.* suggested pre-selecting cells with high expression levels of *SOX9* after a week in culture (15). In their study, this approach increased the success rate and reduced variation. On the other hand, as also observed before (15), *COL10A1* was very lowly expressed at gene expression and protein level, which is characteristic of poor neo-cartilage ECM. Improvement may be established by modifications of the chondrogenic medium, such as by adding BMP2 or BMP4 (13). Finally, when comparing hiMSC- and hPAC-derived neo-cartilage, we can strongly conclude that matrix generated by hiMSC has a hypertrophic phenotype with a 39% similarity to neo-cartilage from primary chondrocytes. This is defined by the lower expression of *COL2A1*(-10.5 fold lower), while *COL1A1*, *ALPL,* and *MMP13* were highly upregulated (5.5, 51.7, and 123.2-fold highly, respectively). The expression of *MMP13* and *ALPL* would suggest a higher collagen degradation with a subsequent calcification, characteristic of terminal chondrogenic differentiation, endochondral ossification and OA initiation (33, 34). Quantification of MMP13 enzymatic activity could help to determine whether the gene expression upregulation also results in an increase of the activate protein (34). The observed differences in neo-cartilage were expected since neo-cartilage from BMSCs and hPAC have a low similarity, and it could be advocated that hiMSCs are an ideal candidate for studying skeletal diseases in which endochondral bone formation and hypertrophy are a driving mechanism (35, 36).

Although hPACs were collected from macroscopically unaffected regions of the articular cartilage, a potential drawback of our study is that they were collected

from patients undergoing joint replacement surgery due to end stage OA. Hence, it could be speculated that, given the higher *COL2A1* and concurrent lower *COL1A1* and *ADAMTS5* levels in hiCPC-derived neo-cartilage, hiCPCs deposit neo-cartilage that is more comparable to healthy cartilage. However, the acquisition of healthy tissue is a challenge in the field, and potential differences between hPACs from preserved and healthy cartilage remain to be determined. Additionally, the emphasis of our manuscript is on the sensitive signaling processes occurring during chondrogenesis. Consequently, further analysis of other significantly different genes and other intrinsic chondrogenic mechanisms would still need to be confirmed by protein expression and ultimately tested in an *in vivo* model.

CONCLUSION

When taking a stepwise approach for chondrogenesis from hiPSCs via chondroprogenitor cells, similarities of almost 70% to primary chondrocytes can be accomplished within 21 days of chondrogenesis. For application of regenerative therapies, this may well be very promising. On the other hand, chondrogenesis methods via hiMSCs result in lower similarity to hPACs, while levels of hypertrophic markers are higher. As such, hiMSCs may be more suitable for *in vitro* models of skeletal diseases.

Acknowledgements

The Leiden University Medical Centre has and is supporting the RAAK study, and we thank all study participants of the RAAK study. We thank Evelyn Houtman, Enrike van der Linden, Robert van der Wal, Peter van Schie, Shaho Hasan, Maartje Meijer, Daisy Latijnhouwers, Anika Rabelink-Hoogenstraaten, and Geert Spierenburg for their contribution to the collection of the joint tissues. We thank all the members of the Molecular Epidemiology Osteoarthritis group for their valuable discussion and feedback. Data is generated within the scope of the Medical Delta programs Regenerative Medicine 4D ("Generating complex tissues with stem cells and printing technology and Improving Mobility with Technology").

Funding

Research leading to these results has received funding from the Dutch Arthritis Society (DAF-16–1-406), the Dutch Scientific Research council NWO/ZonMW VICI scheme (nr 91816631/528), the National Institutes of Health grants AG15768 and AG46927, and from the European Union's Horizon 2020 research and innovation program (No 874671; the material presented and views expressed here are the responsibility of the authors only; the EU Commission takes no responsibility for any use made of the information set out).

Disclosure of potential conflicts of interest

None declared.

Data availability statement

The data that support the funding of this study are available from the corresponding author upon request.

Ethics approval and consent to participate

The Medical Ethics Committee of the LUMC gave approval for the RAAK study (P08.239) and for generation of hiPSCs from skin fibroblasts of healthy donors (P13.080). Informed consent was obtained from all donors.

REFERENCES

1. McKee TJ, Perlman G, Morris M, Komarova SV. Extracellular matrix composition of connective tissues: a systematic review and meta-analysis. Sci Rep. 2019;9(1):10542.
2. Luo Y, Sinkeviciute D, He Y, Karsdal M, Henrotin Y, Mobasheri A, et al. The minor collagens in articular cartilage. Protein Cell. 2017;8(8):560-72.
3. Krishnan Y, Grodzinsky AJ. Cartilage diseases. Matrix Biol. 2018;71-72:51-69.
4. Patel JM, Saleh KS, Burdick JA, Mauck RL. Bioactive factors for cartilage repair and regeneration: Improving delivery, retention, and activity. Acta Biomater. 2019;93:222-38.
5. Stenberg J, de Windt TS, Synnergren J, Hynsjo L, van der Lee J, Saris DB, et al. Clinical Outcome 3 Years After Autologous Chondrocyte Implantation Does Not Correlate With the Expression of a Predefined Gene Marker Set in Chondrocytes Prior to Implantation but Is Associated With Critical Signaling Pathways. Orthop J Sports Med. 2014;2(9):2325967114550781.
6. Ebert JR, Fallon M, Ackland TR, Janes GC, Wood DJ. Minimum 10-Year Clinical and Radiological Outcomes of a Randomized Controlled Trial Evaluating 2 Different Approaches to Full Weightbearing After Matrix-Induced Autologous Chondrocyte Implantation. Am J Sports Med. 2020;48(1):133-42.
7. de Windt TS, Vonk LA, Slaper-Cortenbach ICM, Nizak R, van Rijen MHP, Saris DBF. Allogeneic MSCs and Recycled Autologous Chondrons Mixed in a One-Stage Cartilage Cell Transplantion: A First-in-Man Trial in 35 Patients. Stem Cells. 2017;35(8):1984-93.
8. Bomer N, den Hollander W, Suchiman H, Houtman E, Slieker RC, Heijmans BT, et al. Neo-cartilage engineered from primary chondrocytes is epigenetically similar to autologous cartilage, in contrast to using mesenchymal stem cells. Osteoarthritis Cartilage. 2016;24(8):1423-30.
9. Fellows CR, Matta C, Zakany R, Khan IM, Mobasheri A. Adipose, Bone Marrow and Synovial Joint-Derived Mesenchymal Stem Cells for Cartilage Repair. Front Genet. 2016;7:213.
10. Barry F. MSC Therapy for Osteoarthritis: An Unfinished Story. J Orthop Res. 2019;37(6):1229-35.
11. Liu H, Yang L, Yu FF, Wang S, Wu C, Qu C, et al. The potential of induced pluripotent stem cells as a tool to study skeletal dysplasias and cartilage-related pathologic conditions. Osteoarthritis Cartilage. 2017;25(5):616-24.
12. Nakayama N, Pothiawala A, Lee JY, Matthias N, Umeda K, Ang BK, et al. Human pluripotent stem cell-derived chondroprogenitors for cartilage tissue engineering. Cell Mol Life Sci. 2020;77(13):2543-63.
13. Xu M, Shaw G, Murphy M, Barry F. Induced Pluripotent Stem Cell-Derived Mesenchymal Stromal Cells Are Functionally and Genetically Different From Bone Marrow-Derived Mesenchymal Stromal Cells. Stem Cells. 2019;37(6):754-65.
14. Diederichs S, Tuan RS. Functional comparison of human-induced pluripotent stem cell-derived mesenchymal cells and bone marrow-derived mesenchymal stromal cells from the same donor. Stem Cells Dev. 2014;23(14):1594-610.
15. Diederichs S, Klampfleuthner FAM, Moradi B, Richter W. Chondral Differentiation of Induced Pluripotent Stem Cells Without Progression Into the Endochondral Pathway. Front Cell Dev Biol. 2019;7:270.
16. Nejadnik H, Diecke S, Lenkov OD, Chapelin F, Donig J, Tong X, et al. Improved approach for chondrogenic differentiation of human induced pluripotent stem cells. Stem Cell Rev Rep. 2015;11(2):242-53.
17. Adkar SS, Wu CL, Willard VP, Dicks A, Ettyreddy A, Steward N, et al. Step-Wise Chondrogenesis of Human Induced Pluripotent Stem Cells and Purification Via a Reporter Allele Generated by CRISPR-Cas9 Genome Editing. Stem Cells. 2019;37(1):65-76.
18. Dicks A, Wu CL, Steward N, Adkar SS, Gersbach CA, Guilak F. Prospective isolation of chondroprogenitors from human iPSCs based on cell surface markers identified using a CRISPR-Cas9-generated reporter. Stem Cell Res Ther. 2020;11(1):66.

19. Ramos YF, den HW, Bovee JV, Bomer N, van der Breggen R, Lakenberg N, et al. Genes Involved in the Osteoarthritis Process Identified through Genome Wide Expression Analysis in Articular Cartilage; the RAAK Study. PLoS One. 2014;9(7):e103056.
20. Dambrot C, van de Pas S, van Zijl L, Brandl B, Wang JW, Schalij MJ, et al. Polycistronic lentivirus induced pluripotent stem cells from skin biopsies after long term storage, blood outgrowth endothelial cells and cells from milk teeth. Differentiation. 2013;85(3):101-9.
21. Bomer N, den Hollander W, Ramos YF, Bos SD, van der Breggen R, Lakenberg N, et al. Underlying molecular mechanisms of DIO2 susceptibility in symptomatic osteoarthritis. Ann Rheum Dis. 2015;74(8):1571-9.
22. Dominici M, Le Blanc K, Mueller I, Slaper-Cortenbach I, Marini F, Krause D, et al. Minimal criteria for defining multipotent mesenchymal stromal cells. The International Society for Cellular Therapy position statement. Cytotherapy. 2006;8(4):315-7.
23. Wu CL, Dicks A, Steward N, Tang R, Katz DB, Choi YR, et al. Single cell transcriptomic analysis of human pluripotent stem cell chondrogenesis. Nat Commun. 2021;12(1):362.
24. Seufert DW, Hanken J, Klymkowsky MW. Type II collagen distribution during cranial development in Xenopus laevis. Anat Embryol (Berl). 1994;189(1):81-9.
25. Katz D, Huynh N, Savadipour A, Palte I, Guilak F. An immortalized human adipose-derived stem cell line with highly enhanced chondrogenic properties. Biochemical and Biophysical Research Communications. 2020;530(1):252-8.
26. Fellows CR, Williams R, Davies IR, Gohil K, Baird DM, Fairclough J, et al. Characterisation of a divergent progenitor cell sub-populations in human osteoarthritic cartilage: the role of telomere erosion and replicative senescence. Sci Rep. 2017;7:41421.
27. Kuznetsov SA, Mankani MH, Gronthos S, Satomura K, Bianco P, Robey PG. Circulating skeletal stem cells. J Cell Biol. 2001;153(5):1133-40.
28. Buchert J, Diederichs S, Kreuser U, Merle C, Richter W. The Role of Extracellular Matrix Expression, ERK1/2 Signaling and Cell Cohesiveness for Cartilage Yield from iPSCs. Int J Mol Sci. 2019;20(17).
29. Matta C, Boocock DJ, Fellows CR, Miosge N, Dixon JE, Liddell S, et al. Molecular phenotyping of the surfaceome of migratory chondroprogenitors and mesenchymal stem cells using biotinylation, glycocapture and quantitative LC-MS/MS proteomic analysis. Sci Rep. 2019;9(1):9018.
30. Espagnolle N, Guilloton F, Deschaseaux F, Gadelorge M, Sensebe L, Bourin P. CD146 expression on mesenchymal stem cells is associated with their vascular smooth muscle commitment. J Cell Mol Med. 2014;18(1):104-14.
31. Harkness L, Zaher W, Ditzel N, Isa A, Kassem M. CD146/MCAM defines functionality of human bone marrow stromal stem cell populations. Stem Cell Res Ther. 2016;7:4.
32. Su X, Zuo W, Wu Z, Chen J, Wu N, Ma P, et al. CD146 as a new marker for an increased chondroprogenitor cell sub-population in the later stages of osteoarthritis. J Orthop Res. 2015;33(1):84-91.
33. Chen S, Fu P, Cong R, Wu H, Pei M. Strategies to minimize hypertrophy in cartilage engineering and regeneration. Genes Dis. 2015;2(1):76-95.
34. Li H, Wang D, Yuan Y, Min J. New insights on the MMP-13 regulatory network in the pathogenesis of early osteoarthritis. Arthritis Res Ther. 2017;19(1):248.
35. Kerkhofs J, Leijten J, Bolander J, Luyten FP, Post JN, Geris L. A Qualitative Model of the Differentiation Network in Chondrocyte Maturation: A Holistic View of Chondrocyte Hypertrophy. PLoS One. 2016;11(8):e0162052.
36. Dreier R. Hypertrophic differentiation of chondrocytes in osteoarthritis: the developmental aspect of degenerative joint disorders. Arthritis Res Ther. 2010;12(5):216.

Supplementary Figures

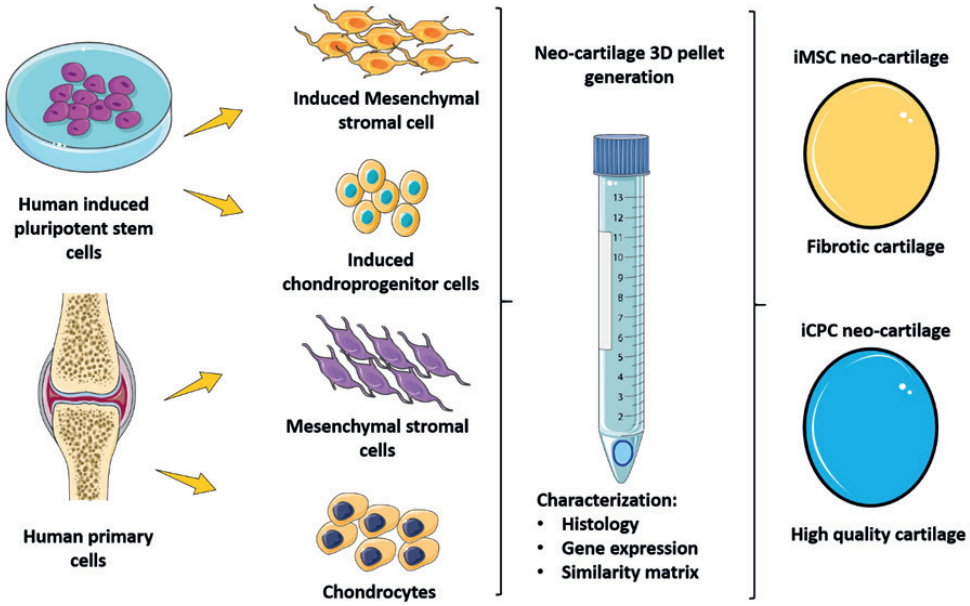

Supplementary Figure S1. Schematic representation of study set up (generated with Servier Medical ART:SMART).

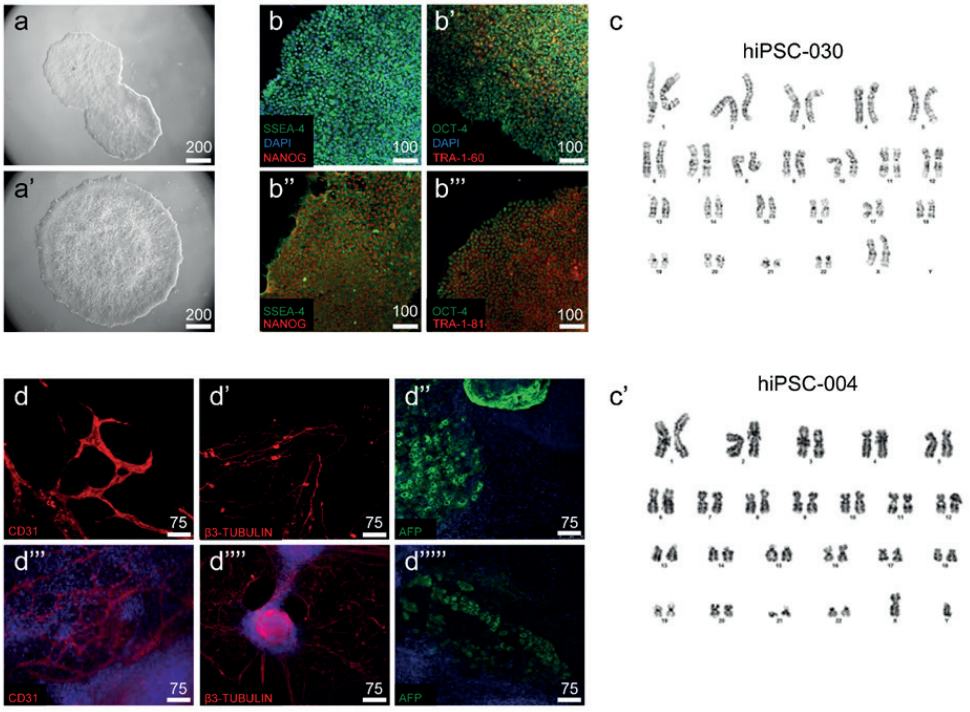

Supplementary Figure S2. Characterization of generated hiPSC control lines. a) Bright field microscopy image of hiPSC colonies. **b**) Immunofluorescent staining for NANOG, TRA-1-60, and TRA-1-81 (red), and SSEA-4 and OCT-4 (green) as indicated in the image. Nuclei are stained with Dapi (blue). **c**) Karyotype demonstrating absence of chromosomal abnormalities. **d**) Expression of CD31, b3-Tubulin, and AFP, as indicated in the image, upon spontaneous differentiation into the three different lineages (mesoderm, ectoderm, and endoderm, respectively). Control line hiPSC-004: **a'**, **b''**, **b'''**, **d'''**, **d''''**, **d'''''**; control line hiPSC-030: **a**, **b**, **b'**, **d**, **d'**, and **d''**.

Supplementary Table S1. Sequences of primers used for RT-qPCR.

	Primer Sequences	
Matrix Genes	**Fwd**	**Rvs**
ACAN	5'AGAGACTCACACAGTCGAAACAGC-3'	5'-CTATGTTACAGTGCTCGCCAGTG-3'
COL2A1	5'-CTACCCCAATCCAGCAAACGT-3'	5'-AGGTGATGTTCTGGGAGCCTT-3'
COL1A1	5' - GTGCTAAAGGTGCCAATGGT-3'	5' -ACCAGGTTCACCGCTGTTAC -3'
COL10A1	5'-GGCAACAGCATTATGACCCA-3'	5'-TGAGATCGATGATGGCACTCC-3'
Hypertrophy genes	**Fwd**	**Rvs**
ADAMTS5	5'-CGTGTACTTGGGCGATGACA-3'	5'-CTGTTGTTGCACACCCCTCT-3'
MMP13	5'-TTGAGCTGGACTCATTGTCG-3'	5'-GGAGCCTCTCAGTCATGGAG-3'
EPAS1	5'-ACAGGTGGAGCTAACAGGAC-3'	5'-CCGTGCACTTCATCCTCATG-3'
WWP2	5'-CACATGTGTCTCCTGGTCCC-3'	5'-GGCAGGGGAAGTGTGCATAT-3'
ALPL	5'-CAAAGGCTTCTTCTTGCTGGTG-3'	5'-CCTGCTTGGCTTTTCCTTCA-3'
Chondrogenesis genes	**Fwd**	**Rvs**
SOX5	5'-CCTCAAAGCCTCTGTCCCAG-3'	5'-TGCCTTGGTGACAGCATCAT-3'
SOX6	5'-AACAACGGCAGCAAATGGAC-3'	5'-TGGATCTGTTGCTGCAGGAG-3'
SOX9	5'-CCCCAACAGATCGCCTACAG-3'	5'-CTGGAGTTCTGGTGGTCGGT-3'
FGFR2	5'-TCTCTTCAACGGCAGACACC-3'	5'-AAAGCAACCTTCTCCCAGGG-3'
NOTCH1	5'-AGGACTGCAGCGAGAACATT-3'	5'-GCAGTAGAAGGAGGCCACAC-3'
NOTCH3	5'-GTGGATGGCGTCAACACCTA-3'	5'-CTGCAGCTGACACTCATCCA-3'
SMAD3	5'-GCCCCTTTCAGGTAACCGTC-3'	5'-GAAGCGGCTGATGCTCCTTA-3'
SMAD7	5'- CGAATTATCTGGCCCCTGGG-3'	5'-TCCCCACTCTCGTCTTCTCC-3'
GDF5	5'-GACATGGTCGTGGAGTCGTG-3'	5'-CCCCTCTGTGATTCCAGGAGT-3'
PRG4	5'-AAAGTCAGCACATCTCCCAAG-3'	5'-GTGTCTCTTTAGCGGAAGTAGTC-3'
NFAT5	5'-AGGCCTGCAGAGTAACTGGA-3'	5'-CCGCCAGTGTCATGTTGTTG-3'
Housekeeping genes	**Fwd**	**Rvs**
GAPDH	5'-TGCCATGTAGACCCCTTGAAG-3'	5'-ATGGTACATGACAAGGTGCGG-3'
ARP	5'-CACCATTGAAATCCTGAGTGATGT-3'	5'-TGACCAGCCGAAAGGAGAAG-3'

Supplementary Table S2. Similarity tables for the different samples included in the current study.

Similarity table BMSCs against iMSCs (a)

	BMSC1	BMSC2	BMSC3	BMSC4	BMSC5	iMSC1	iMSC2	iMSC3	iMSC4	iMSC5	iMSC6	iMSC7
BMSC1	1.0	0.9	0.7	0.9	0.8	0.4	0.3	0.3	0.6	0.6	0.6	0.7
BMSC2	0.9	1.0	0.9	0.9	0.8	0.5	0.4	0.4	0.7	0.7	0.7	0.6
BMSC3	0.7	0.9	1.0	0.7	0.9	0.6	0.6	0.6	0.8	0.5	0.6	0.8
BMSC4	0.9	0.9	0.7	1.0	0.7	0.4	0.2	0.2	0.4	0.6	0.6	0.4
BMSC5	0.8	0.8	0.9	0.7	1.0	0.6	0.4	0.5	0.7	0.4	0.4	0.8
iMSC1	0.4	0.5	0.6	0.4	0.6	1.0	0.7	0.8	0.6	0.6	0.6	0.6
iMSC2	0.3	0.4	0.6	0.2	0.4	0.7	1.0	0.8	0.7	0.7	0.7	0.7
iMSC3	0.3	0.4	0.6	0.2	0.5	0.8	0.8	1.0	0.6	0.5	0.5	0.6
iMSC4	0.6	0.7	0.8	0.4	0.7	0.6	0.7	0.6	1.0	0.5	0.6	0.8
iMSC5	0.6	0.7	0.5	0.6	0.4	0.6	0.7	0.5	0.5	1.0	1.0	0.6
iMSC6	0.6	0.7	0.6	0.6	0.4	0.6	0.7	0.5	0.6	1.0	1.0	0.6
iMSC7	0.7	0.6	0.8	0.4	0.8	0.6	0.7	0.5	0.8	0.6	0.6	1.0

Similarity table hPACs against iCPCs (b)

	hPAC1	hPAC2	hPAC3	hPAC4	hPAC5	hPAC6	hPAC7	hPAC8	hPAC9	iCPC1	iCPC2	iCPC3	iCPC4	iCPC5	iCPC6
hPAC1	1.0	0.9	0.9	0.9	0.9	0.9	0.8	0.7	0.9	0.7	0.6	0.7	0.6	0.8	0.8
hPAC2	0.9	1.0	1.0	0.7	0.8	0.7	0.6	0.6	0.8	0.6	0.5	0.5	0.5	0.7	0.8
hPAC3	0.9	1.0	1.0	0.8	0.8	0.8	0.7	0.6	0.9	0.7	0.6	0.6	0.6	0.8	0.8
hPAC4	0.9	0.7	0.8	1.0	0.9	0.9	0.9	0.9	0.9	0.8	0.6	0.7	0.7	0.8	0.8
hPAC5	0.9	0.8	0.8	0.9	1.0	0.8	0.7	0.7	0.8	0.7	0.5	0.7	0.6	0.7	0.8
hPAC6	0.9	0.7	0.8	0.9	0.8	1.0	0.8	0.8	0.9	0.6	0.5	0.7	0.5	0.7	0.7
hPAC7	0.8	0.6	0.7	0.9	0.7	0.8	1.0	1.0	0.8	0.7	0.6	0.7	0.6	0.7	0.8
hPAC8	0.7	0.6	0.6	0.9	0.7	0.8	1.0	1.0	0.7	0.7	0.6	0.7	0.6	0.7	0.7
hPAC9	0.9	0.8	0.9	0.9	0.8	0.9	0.8	0.7	1.0	0.7	0.5	0.7	0.6	0.6	0.6
iCPC1	0.7	0.6	0.7	0.8	0.7	0.6	0.7	0.7	0.7	1.0	0.9	0.8	0.7	0.9	0.9

Similarity table hPACs against iCPCs (b)															
	hPAC1	**hPAC2**	**hPAC3**	**hPAC4**	**hPAC5**	**hPAC6**	**hPAC7**	**hPAC8**	**hPAC9**	**iCPC1**	**iCPC2**	**iCPC3**	**iCPC4**	**iCPC5**	**iCPC6**
iCPC2	0.6	0.5	0.6	0.6	0.5	0.5	0.6	0.6	0.5	0.9	1.0	0.8	0.7	0.9	0.8
iCPC3	0.7	0.5	0.6	0.7	0.7	0.7	0.7	0.7	0.7	0.8	0.8	1.0	0.7	0.8	0.8
iCPC4	0.6	0.5	0.6	0.7	0.6	0.5	0.6	0.6	0.6	0.7	0.7	0.7	1.0	0.7	0.6
iCPC5	0.8	0.7	0.8	0.8	0.7	0.7	0.7	0.7	0.6	0.9	0.9	0.8	0.7	1.0	0.9
iCPC6	0.8	0.8	0.8	0.8	0.8	0.7	0.8	0.7	0.6	0.9	0.8	0.8	0.6	0.9	1.0

Similarity table hPACs against iMSCs (c)																
	hPAC1	**hPAC2**	**hPAC3**	**hPAC4**	**hPAC5**	**hPAC6**	**hPAC7**	**hPAC8**	**hPAC9**	**iMSC1**	**iMSC2**	**iMSC3**	**iMSC4**	**iMSC5**	**iMSC6**	**iMSC7**
hPAC1	1.0	0.9	0.9	0.9	0.9	0.9	0.8	0.7	0.9	0.3	0.6	0.6	0.1	0.2	0.1	0.5
hPAC2	0.9	1.0	1.0	0.8	0.8	0.7	0.6	0.6	0.8	0.2	0.5	0.5	0.1	0.2	0.1	0.4
hPAC3	0.9	1.0	1.0	0.8	0.8	0.8	0.7	0.6	0.9	0.2	0.6	0.6	0.1	0.2	0.0	0.4
hPAC4	0.9	0.8	0.8	1.0	0.9	0.9	0.9	0.9	0.9	0.5	0.7	0.7	0.3	0.4	0.3	0.6
hPAC5	0.9	0.8	0.8	0.9	1.0	0.8	0.7	0.7	0.8	0.4	0.6	0.6	0.2	0.3	0.3	0.6
hPAC6	0.9	0.7	0.8	0.9	0.8	1.0	0.8	0.8	0.9	0.4	0.5	0.5	0.2	0.4	0.2	0.6
hPAC7	0.8	0.6	0.7	0.9	0.7	0.8	1.0	1.0	0.8	0.4	0.7	0.7	0.3	0.4	0.3	0.6
hPAC8	0.7	0.6	0.6	0.9	0.7	0.8	1.0	1.0	0.7	0.5	0.7	0.7	0.4	0.5	0.4	0.6
hPAC9	0.9	0.8	0.9	0.9	0.8	0.9	0.8	0.7	1.0	0.1	0.5	0.5	0.0	0.2	0.0	0.5
iMSC1	0.5	0.2	0.2	0.5	0.4	0.4	0.4	0.5	0.1	1.0	0.6	0.6	0.7	0.9	0.8	0.7
iMSC2	0.6	0.5	0.6	0.7	0.6	0.5	0.7	0.7	0.5	0.6	1.0	1.0	0.5	0.7	0.5	0.5
iMSC3	0.6	0.5	0.6	0.7	0.6	0.5	0.7	0.7	0.5	0.6	1.0	1.0	0.6	0.7	0.5	0.5
iMSC4	0.1	0.1	0.1	0.3	0.2	0.2	0.3	0.4	0.0	0.7	0.5	0.6	1.0	0.7	0.7	0.6
iMSC5	0.2	0.2	0.2	0.4	0.3	0.4	0.4	0.5	0.2	0.9	0.7	0.7	0.7	1.0	0.8	0.7
iMSC6	0.1	0.1	0.0	0.3	0.3	0.2	0.3	0.4	0.0	0.8	0.5	0.5	0.7	0.8	1.0	0.8
iMSC7	0.5	0.4	0.4	0.6	0.6	0.6	0.6	0.6	0.5	0.7	0.5	0.5	0.6	0.7	0.8	1.0

Supplementary Table S3. Differences in gene expression between hiCPC-derived neo-cartilage at week 3 and 5. Significant differential expression depicted in bold.

hiCPCs week 3 versus week 5				
Matrix genes	**FD**	**Beta**	**SE**	**P value**
ACAN	-5.1	-2.8	1.7	$1.0x10^{-1}$
COL2A1	-4.7	-2.7	1.6	$9.3x10^{-2}$
COL1A1	-1.2	-0.3	0.8	$7.5x10^{-1}$
COL10A1	-2.4	-1.6	1.1	$1.5x10^{-1}$
Hypertrophy genes	**FD**	**Beta**	**SE**	**P value**
ADAMTS5	-3.4	-2.1	1.3	$9.4x10^{-2}$
MMP13	-1.2	-0.3	2.0	$8.9x10^{-1}$
EPAS1	-5.0	-2.8	1.7	$1.1x10^{-1}$
WWP2	-1.1	-0.2	0.4	$5.4x10^{-1}$
ALPL	**4.3**	**2.5**	**1.1**	$\mathbf{1.8x10^{-2}}$
Chondrogenesis genes	**FD**	**Beta**	**SE**	**P value**
SOX5	-1.5	-0.7	0.5	$1.7x10^{-1}$
SOX6	2.0	1.2	1.4	$3.7x10^{-1}$
SOX9	-1.1	-0.2	0.8	$8.0x10^{-1}$
FGFR2	-1.4	-0.6	0.7	$3.4x10^{-1}$
NOTCH1	1.0	0.0	0.6	$9.6x10^{-1}$
NOTCH3	1.4	0.5	0.3	$6.5x10^{-2}$
SMAD3	1.5	0.7	1.0	$4.4x10^{-1}$
SMAD7	3.2	2.0	1.4	$1.5x10^{-1}$
GDF5	-1.4	-0.6	1.2	$6.2x10^{-1}$
PRG4	-1.3	-0.4	0.7	$5.0x10^{-1}$
NFAT5	-1.3	-0.5	0.4	$2.1x10^{-1}$